



Published in final edited form as:

Pharm Res. 2016 August ; 33(8): 1959–1971. doi:10.1007/s11095-016-1932-2.

## The Evaluation Of Therapeutic Efficacy and Safety Profile of Simvastatin Prodrug Micelles in a Closed Fracture Mouse Model

Yijia Zhang<sup>a,§</sup>, Zhenshan Jia<sup>a,§</sup>, Hongjiang Yuan<sup>a</sup>, Anand Dusad<sup>a</sup>, Ke Ren<sup>a</sup>, Xin Wei<sup>a</sup>, Edward V. Fehring<sup>b</sup>, P. Edward Purdue<sup>c</sup>, Aaron Daluiski<sup>c</sup>, Steven R. Goldring<sup>c</sup>, and Dong Wang<sup>a,b,\*</sup>

<sup>a</sup>Department of Pharmaceutical Sciences, University of Nebraska Medical Center, Omaha, NE, 68198, USA

<sup>b</sup>Department of Orthopaedic Surgery and Rehabilitation, University of Nebraska Medical Center, Omaha, NE, 68198, USA

<sup>c</sup>Hospital for Special Surgery, New York, NY, 10021, USA

### Abstract

**Purpose**—To evaluate the therapeutic efficiency of a micellar prodrug formulation of simvastatin (SIM/SIM-mPEG) and explore its safety in a closed femoral fracture mouse model.

**Methods**—The amphiphilic macromolecular prodrug of simvastatin (SIM-mPEG) was synthesized and formulated together with free simvastatin into micelles. It was also labeled with a near infrared dye for *in vivo* imaging purpose. A closed femoral fracture mouse model was established using a three-point bending device. The mice with established closed femoral fracture were treated with SIM/SIM-mPEG micelle, using free simvastatin and saline as controls. The therapeutic efficacy of the micelles was evaluated using a high-resolution micro-CT. Serum biochemistry and histology analyses were performed to explore the potential toxicity of the micelle formulation.

**Results**—Near Infrared Fluorescence (NIRF) imaging confirmed the passive targeting of SIM/SIM-mPEG micelles to the bone lesion of the mice with closed femoral fracture. The micelle was found to promote fracture healing with an excellent safety profile. In addition, the accelerated healing of the femoral fracture also helped to prevent disuse-associated same-side tibia bone loss accompanying the femur fracture.

**Conclusion**—SIM/SIM-mPEG micelle was found to be an effective and safe treatment for closed femoral fracture repair in mice. The evidence obtained in this study suggests that it may have the potential to be translated into a novel therapy for clinical management of skeletal fractures and non-union.

\*Corresponding author: 986025 Nebraska Medical Center, COP 3026, Omaha, Nebraska 68198-6025, USA. Tel.: +1 402 559 1995, Fax: +1 402 559 9543. dwang@unmc.edu (D. Wang).

§These authors contributed equally to this work.

### DISCLOSURES

Y.Z., Z.J., A.D., S.R.G. and D.W. are listed as co-inventors in a PCT patent application filed for the SIM/SIM-mPEG prodrug micelle technology.

## Keywords

Fracture; micelle; prodrug; simvastatin; ELVIS

---

## 1. INTRODUCTION

Among the most common of musculoskeletal injuries, fractures continue to pose a major social and economic burden to our society. It has been projected that by 2025, there will be over 3 million fractures in the US, with related expenditures of \$25.3 billion per year (1, 2). Despite significant advances in the development of bone active therapeutics in the past few decades, there is still an urgent need for more effective treatments for impaired fracture healing.

Simvastatin (SIM), a widely used anti-lipidaemic drug, has been identified as a bone anabolic agent. Its poor water solubility and the lack of distribution to the skeleton, however, have limited its applications in the treatment of bone metabolic diseases (3). By employing a drug delivery strategy, some local applications of statins have shown promise in the treatment of accessible bony defects (4, 5). The utility of this strategy, however, requires accessibility to the pathologies during the surgery. For fractures at anatomical locations such as rib, wrist, pelvis, etc., which do not always justify surgical intervention, and/or for trauma patients with multiple fractures, a systemic administration of bone anabolic agents that would specifically concentrate at the fracture lesions to augment bone healing and regeneration would be ideal. Such systemic treatment may also help to mitigate the potential risk that often is associated with a local surgical approach. Recently, in a proof-of-concept study, we designed and synthesized an amphiphilic macromolecular prodrug of SIM (SIM-mPEG) to overcome the limitations seen in systemic applications of the drug (6). The prodrug consists of a SIM trimer as the hydrophobic segment and a methoxy polyethylene glycol (mPEG) as the hydrophilic segment. This amphiphilic prodrug can spontaneously self-assemble into micelles. Due to the structural similarity to the SIM trimer, free SIM can be readily incorporated into the hydrophobic core of the micelle to increase the micelle stability and payload. In addition, the concomitant physical and chemical loading of SIM in the micelle may also provide an *in vivo* drug releasing profile consisting of both an initial fast drug release from the physical entrapment and a sustained drug release from activation of the chemical conjugated payload. In our previous proof-of-concept study, it was demonstrated that this systemically-delivered micellar formulation of SIM prodrug (SIM/SIM-mPEG) passively targeted the bone fracture site via the ELVIS (Extravasation through Leaky Vasculature and Inflammatory cell-mediated Sequestration) mechanism (6–10) and promoted fracture healing in an open fracture mouse model (6).

However, the relevant dosing level of SIM used in the previous study was considered high (11) in either free drug or micellar formulation. As a potential sign of toxicity in one of our pilot studies, significant body weight loss was found with the free SIM-treated mice (6 mg/kg/d) at the experimental endpoint, compared to the vehicle-treated and SIM/SIM-mPEG-treated groups. Clearly, the dosing schedule and dosing level need to be further optimized to limit toxicity and meet the safety requirements.

Clinically, closed fractures are more common than open fractures. To further investigate potential clinical applications of SIM/SIM-mPEG in closed fractures, we established a mouse closed fracture model using a three-point bending device, evaluated the safety and therapeutic efficacy of SIM/SIM-mPEG micelles in this model, and developed an optimized dosing schedule.

## 2. EXPERIMENTAL SECTION

### 2.1 Materials

Simvastatin was purchased from Zhejiang Ruibang Laboratories (Wenzhou, Zhejiang, China). IRDye<sup>®</sup> 800CW NHS ester was purchased from LI-COR Biosciences (Lincoln, NE, USA). SIM-mPEG (Scheme 1) and IRDye<sup>®</sup> 800CW labeled SIM-mPEG were synthesized according to procedures described previously (6). All other reagents and solvents were purchased from Acros Organics (Morris Plains, NJ, USA) and used as received.

Ten-week-old male CD-1 mice were purchased from Charles River Laboratories, and maintained under standard housing conditions. All animal experiments were performed in accordance with guidelines evaluated and approved by the Institutional Animal Care and Use Committee (IACUC) of University of Nebraska Medical Center.

### 2.2 Mouse closed fracture model

All mice underwent a standardized, unilateral closed transverse femoral mid-shaft fracture. Under anesthesia with isoflurane, the mouse's right hips, thighs, and knees were prepared with povidone-iodine solution. A 3-mm medial parapatellar incision was created. The patella was dislocated to expose the femoral condyles. A hole was drilled into the femoral intramedullary canal at the intercondylar notch using a 25-gauge needle. A 25-gauge needle was inserted into the intramedullary canal to stabilize the impending fracture. The patella was then reduced, and the incision was closed in 2 layers using 4-0 synthetic absorbable suture for the arthrotomy and non-absorbable suture for skin closure. The non-absorbable sutures were removed 10–14 days after surgery. Immediately after the pin implantation, a closed diaphyseal fracture was produced in the right femur using a modified method described by Bonnarens and Einhorn with a three-point bending device (12). A highly reproducible transverse fracture was created with minimal comminution and minimal angulation of the intramedullary pin. Animals were imaged with an X-ray imaging system (Faxitron MX-20, Tucson, AZ) post fracture to verify that a mid-diaphyseal fracture had been produced. The animals were allowed free, unrestricted weight bearing after recovery from anesthesia.

Postoperatively, twice-daily antibiotic (cefazolin sodium, 25 mg/kg, s.c.) and analgesia (buprenorphine, 0.1 mg/kg, s.c.) were given for three days following surgery. Animals were closely monitored for fractured limb function and general postoperative health. Body weight was recorded weekly.

### 2.3 *In vivo* imaging

NIRF optical imaging was performed to observe the *in vivo* biodistribution of the SIM/SIM-mPEG micelles after its systemic administration in the closed fracture mouse model. At 7-day post surgery, the mice were shaved and given IRDye<sup>®</sup> 800CW-labeled SIM/SIM-mPEG (SIM-PEG-IRDye, 1 mg/mouse, n=3) via tail vein injection. The mice were imaged prior to and then daily after imaging agent injection using a Pearl<sup>™</sup> *In Vivo* Imaging System (LICOR Biosciences, Lincoln, NE, USA) to evaluate the distribution of the SIM/SIM-mPEG continuously for the 7 days. All of the mice were scanned under anesthesia with isoflurane (inhalational 1%~1.5%, Piramal Healthcare, Andhra Pradesh, India). The images were captured using channels 800 and white with the resolution of 170  $\mu\text{m}$  at focus position 2. The NIRF signal intensity was measured semi-quantitatively at a consistent region of interest (ROI) at the fractured and the contralateral intact leg for all mice.

### 2.4 Preparation of SIM/SIM-mPEG Micelles

The film hydration method was used as described previously (6). For each weekly i.v. administration, simvastatin was dissolved in a methanol solution of SIM-mPEG conjugate (1 mL). Methanol was then removed by rotor evaporation at 60°C to form a film of the drug and polymeric prodrug. To completely remove the solvent residue, the film was placed in vacuum overnight. To prepare the micelles, the film was hydrated with 2 mL of saline at room temperature for 30 min. The undissolved drug was removed by centrifugation at 12,000 rpm for 0.5 min, followed by filtration of the supernatant through a 0.2  $\mu\text{m}$  filter. This micelle solution (0.2 mL, equiv. 21 mg/kg/wk or 42 mg/kg/wk of simvastatin) was given to the mice weekly via tail vein injection.

### 2.5 Preparation of Simvastatin Acid

To obtain simvastatin acid (SIMA) as a water-soluble free SIM control, sodium hydroxide (0.1 N, 9 mL) was added to a SIM solution in ethanol (6 mL, 42 g/L). The resulting solution was stirred at 50°C for 2 h to hydrolyze the lactone ring of simvastatin. Residual ethanol was removed under vacuum. The resulting solution was neutralized to pH 6.0 with HCl (0.1 M) and then was lyophilized. The resulting dry powder was dispersed in acetone and centrifuged to remove NaCl. SIMA was then isolated from the supernatant via rotor evaporation (13). For daily i.p. dosing, 1.25 or 2.5 mg of SIMA was dissolved into saline (1 mL) to obtain the final injectable solution. This solution (0.1 mL, equiv. 3 or 6 mg/kg/d of simvastatin) was given to animals daily via i.p. injection.

The chemical structure and purity of SIM-mPEG and simvastatin acid were confirmed by thin layer chromatography (TLC) and <sup>1</sup>H NMR.

### 2.6 Safety evaluation

A preliminary toxicity study was conducted to optimize the dosage of SIM used in SIM/SIM-mPEG. Male CD-1 mice were randomly assigned into four groups (n = 6): SIM/SIM-mPEG Low dose (equiv. SIM 3 mg/kg/d or 21 mg/kg/wk, weekly i.v.), SIM/SIM-mPEG High dose (equiv. SIM 6 mg/kg/d or 42 mg/kg/wk, weekly i.v.), SIM (SIMA 6 mg/kg/d, daily i.p.) and vehicle-treated control group (CON). The treatments were initiated on day 7 post surgery and the mice were euthanized on day 21 (Scheme 2). At the experimental

endpoint, blood samples were collected and centrifuged at 3000 rpm for 10 min within 1 h after collection. The serums were stored in the  $-80^{\circ}\text{C}$  freezer before they were analyzed. Serum biochemistry panel including aspartate aminotransferase (AST), alanine aminotransferase (ALT), alkaline phosphatase (ALP), creatine phosphokinase (CPK), glucose, total protein (TP), albumin, blood urea nitrogen (BUN), creatinine, total bilirubin, calcium and sodium were evaluated by the Clinical Research Center Research Laboratory at Nebraska Medical Center. The major organs (e.g. heart, lung, liver, spleen and kidney) were also collected for the histopathologic evaluation when needed. The specimens were fixed, paraffin-embedded, sectioned and stained with hematoxylin and eosin (H&E) (Sigma-Aldrich, St. Louis, MO) and analyzed using light microscopy.

## 2.7 Therapeutic efficacy study

Male CD-1 mice were randomly assigned into four groups ( $n = 10$ ): SIM/SIM-mPEG (equiv. SIM 3 mg/kg/d or 21 mg/kg/wk, weekly i.v.), SIM (SIMA 3 mg/kg/d, daily i.p.), SIM-H (SIMA 6 mg/kg/d daily i.p.) and a vehicle-treated control group (CON). The treatments were initiated on day 2 post surgery and the mice were euthanized on day 21 (Scheme 3). The body weight of all mice was monitored weekly.

## 2.8 Micro-CT imaging and analysis of the fractured femur

At necropsy, the fractured femurs were collected, fixed in 10% formalin and processed for further micro-CT imaging and analysis (Bruker SkyScan1172, Kontich, Belgium). Each femur was scanned and reconstructed into a 3D-structure with a voxel size of  $5.5\ \mu\text{m}$ . The X-ray tube voltage was 70 kV and the current was  $141\ \mu\text{A}$ , with a 0.5 mm thick aluminum filter. Exposure time was 530 ms. The X-ray projections were obtained at  $0.7^{\circ}$  intervals with a scanning angular rotation of  $180^{\circ}$  and eight frames were averaged for each rotation. 3D reconstructions were performed using NRecon software.

For the quantitative analysis, we specifically focused on the site of fracture callus formation. The position of each bone was corrected with DataViewer and then saved on a volume of interest (VOI) of 400 slices (resized by 2). This was followed by careful placement of a constant square region of interest (ROI) in the callus with 200 slices above and below the fracture line. To standardize analysis within the animals, special care was taken so as to keep the constant ROI in the center for each sample, with the fracture line and metal rod (fixation needle) serving as horizontal and vertical points of reference, respectively. A custom analysis process was performed with a series of specific threshold settings in CTan (MicroPhotonic) and these were kept constant for all samples. The following parameters were measured and calculated: callus bone volume fraction (BV/TV) and callus bone surface density (BS/TV) etc. For non-metric indices, connectivity density (Conn.D) and mean polar moment of inertia (MMI) were also analyzed. While the total callus volume and the total mineralized callus tissue volumes are of great interests, the above analysis protocol was selected due to the large variation of the callus shape/volume.

## 2.9 Micro-CT analysis of the non-fractured tibia

The tibias from the loaded (intact) side and the unloaded (fracture) side were also collected, fixed and then scanned using micro-CT with the following scanning settings: voltage 48 kV,

current 189  $\mu$ A, exposure time 580 msec, resolution 6.0  $\mu$ m with an aluminum filter of 0.5 mm. Three-dimensional reconstructions were performed with NRecon software and then further reoriented with DataViewer software. The proximal metaphyseal regions of the trabecular bone was selected for analysis based on a polygonal region of interest within the cortical bone of the tibia in the transverse section, starting at 40 slices (0.48 mm) distal from the growth plate reference and extending distally 100 slices (1.2 mm) further. 3D morphometric parameters i.e. bone mineral density (BMD), trabecular bone volume fraction (BV/TV), trabecular number (Tb.N), and trabecular thickness (Tb.Th), trabecular separation (Tb.Sp), trabecular bone surface density (BS/TV), trabecular bone pattern factor (Tb.Pf), structure model index (SMI), fractal dimension (FD), degree of anisotropy (DA) and 2D morphometric parameters i.e. mean eccentricity (Ecc), mean polar moment of inertia (MMI) were quantified with CTan software.

### 2.10 Statistical analysis

For the quantitative analysis of micro-CT, data is expressed as mean  $\pm$  SD. Statistical analysis was done by one-way analysis of variance (ANOVA) with LSD/Tamhane's T2 test as post-hoc test. A value of  $P < 0.05$  was considered statistically significant.

## 3. RESULTS

### 3.1 *In vivo* targeting of SIM/SIM-mPEG's in the closed fracture mouse model

To investigate the targeting and retention of SIM/SIM-PEG micelles at the closed fracture site, IRDye<sup>®</sup> 800CW-labeled SIM-PEG was synthesized as described previously and utilized as a probe to visualize the biodistribution. Both of the supine and prone positions of the animals were utilized in the entire optical imaging study. Compared to the intact sides, fractured sides demonstrated more intense and sustained (up to 6 days) NIR signals in the femoral region (Figure 1), consistent with preferential uptake and retention of the SIM/SIM-PEG in the fracture callus. Semi-quantitative analysis of the fluorescent signal intensity at the ROI confirmed the visual observation of the micelle's passive targeting and retention at the fracture site. Due to the renal clearance of the micelle, NIR signals from the kidney and bladder were observed concurrently with the signal at the fractured femur. Potential NIR signals from liver were also observed at the beginning of this study.

### 3.2 Toxicological evaluation of SIM/SIM-mPEG micelles in a closed fracture mouse model

As shown in Figure 2, serum biomarkers including aspartate aminotransferase (AST), alkaline phosphatase (ALP), creatine phosphokinase (CPK), glucose, total protein (TP), albumin, blood urea nitrogen (BUN), creatinine, total bilirubin, calcium and sodium were not significantly changed by the administration of SIM or SIM/SIM-mPEG indicating no evidence of toxicity in the major organs e.g. kidney, cardiac muscle and islet cells in the pancreas. However, 42 mg/kg/wk of SIM/SIM-mPEG induced a significant increase in alanine aminotransferase (ALT) levels when compared to CON. Despite no significant signs of toxicity in the follow-up histopathologic evaluation of the liver (Figure 3), this finding suggested that the optimal dosage of SIM in SIM/SIM-mPEG formulation should be adjusted to be lower than 42 mg/kg/wk. A 21 mg/kg/wk dose was therefore used in the following efficacy study.

### 3.3 Therapeutic efficacy of SIM/SIM-mPEG micelles in the closed fracture mouse model

As shown in Figure 4, after the treatment, the SIM/SIM-mPEG-treated group exhibited greater mineralization of the fracture callus. In contrast, the CON- and SIM-treated group demonstrated less mineralized callus formation at the fracture site (shown as dark areas or cavities in Figure 4). Quantitative analysis of the micro-CT data further validates this observation. As shown in Figure 5, micro-CT morphometric parameters, including callus bone volume (BV), bone volume fraction (BV/TV), callus bone surface density (BS/TV), connectivity density (Conn.D) and mean polar moment of inertia (MMI) were all significantly higher in the SIM/SIM-mPEG group compared to the CON mice ( $P < 0.003$ ), consistent with enhanced callus formation, organization and strength. For the SIM group, these parameters (except Conn.D) were significantly lower compared to the SIM/SIM-mPEG treated group ( $P < 0.05$ ). No significant differences were found between SIM and CON groups. Compared to the CON group, the SIM-H treated group showed significant increases only in BS and Conn.Dn.

### 3.4 SIM/SIM-mPEG treatment can attenuate tibial bone loss due to fracture associated unloading

As shown in Figure 6, the vehicle control-treated group demonstrated a significant decline ( $P < 0.05$ ) of BMD and bone volume fraction (BV/TV) in the unloaded tibia (from fractured side) vs. loaded tibia (from non-fractured side), suggesting that the closed fracture procedures could lead to disuse of the fractured limb and subsequent unloading-associated bone loss in the proximal metaphyseal region of the tibias. No significant difference between loaded and unloaded sides was found for the SIM/SIM-mPEG treated group, suggesting that the SIM/SIM-mPEG may be able to prevent disuse-associated bone loss. Dose equivalent or even double the equivalent doses in the SIM-treated group could not attenuate this bone loss.

As shown in Figure 7, the quantitative analysis of the tibial (fractured side) micro-CT data convincingly showed that SIM/SIM-mPEG treatment efficiently preserved the bone volume fraction (BV/TV), bone mineral density (BMD), trabecular number (Tb.N), trabecular bone surface density (BS/TV) and fractal dimension (FD) with significantly higher values than those observed for the vehicle control, and even significantly higher than that observed for the animals treated with free SIM at the same or double the equivalent dosage. The opposite pattern was found in the measurement of trabecular bone pattern factor (Tb.Pf) and structure model index (SMI), indicating the SIM/SIM-mPEG treated mice had better connectivity and structural complexity of the trabecular network.

## 4. DISCUSSION

Statins, such as simvastatin (SIM), are 3-hydroxy-3-methylglutaryl (HMG)-CoA reductase inhibitors that have been used extensively in clinical management of lipid metabolism, benefiting the prevention/treatment of cardiovascular diseases. Since Mundy et al. (14) first reported the bone anabolic effects of statins, extensive efforts have been invested in understanding the working mechanism and validating the anabolic effect of statins in humans. The basic mechanistic findings obtained so far have suggested that the statins exert their bone anabolic effects by differentiating mesenchymal cells into osteoblasts via up-

regulating BMP-2 and protecting osteoblasts from apoptosis. In addition, statins have been suggested to be anti-osteoclastic by reducing the osteoclast differentiation and activity (3, 15). The statins were originally designed as hepatotropic agents to target cholesterol metabolism. In clinical use, their systemic administration to stimulate bone anabolism has been limited by the requirement for the use of high doses of these agents, which result in significant unacceptable hepatotoxicity.

A potential solution to this challenging problem would be to modify the' pharmacokinetics/ biodistribution (PK/BD) profiles of the statins, favoring a sustained preferential distribution to the skeletal lesions. In a previous study, we have reported the development and *in vivo* evaluation of this macromolecular prodrug micelle formulation of SIM (6) and showed that it passively targeted the fracture site and accelerated the healing process based on rigorous histopathological evaluation, cellular characterization and  $\mu$ CT analysis. An osteotomy procedure was utilized in the previous study to establish an open fracture model under visible control (16). While the fracture location and the fracture line are well controlled, this procedure produces significant soft tissue trauma that may disrupt the vascularization at the fracture site (17). In contrast, the closed fracture method does not require surgical exposure except the intramedullary fixation. The anatomical position of the bone is determined by palpation and the fracture is established by applying external force to the bone, using a three-point bending device as described in this study. This approach only produces minor soft tissue injury (12, 16, 18, 19).

To better recapitulate the clinical events of fracture injury and to further validate SIM/SIM-mPEG micelle's therapeutic benefits, we have extended the initial observations in the open fracture model to evaluate the micelle formulation in a closed fracture model. The micelle dosing level was also optimized according to the feedback from our toxicity study.

As shown in Figure 1, systemically-administrated SIM/SIM-mPEG micelles can passively target the closed fracture site. Similar to the inflammation-targeting we observed in the open fracture mouse model (6), the ELVIS mechanism (Extravasation through Leaky Vasculature and Inflammatory cell-mediated Sequestration) (7–10, 20) provides a pathological window to allow the nano-formulations of SIM to target and be retained at the closed fracture site. Since bony and some muscle trauma occur while performing closed fractures (18, 19), the leaky vasculature associated with the hematoma and acute inflammation allows the extravasation of systemically administered colloids (i.e. SIM/SIM-mPEG micelle), which will then be sequestered by the inflammatory infiltrates and activated resident cells at the fracture site as demonstrated in the previous study (6).

In the toxicity study, all the tested compounds were generally well tolerated except SIM/SIM-mPEG micelle dosed at 42 mg/kg/wk. At this level, a significant increase in serum alanine aminotransferase (ALT) level was observed when compared to the CON group. Significantly elevated ALT levels may be indicative of potential liver toxicity. Even though no histological evidence of liver damage was detected (Figure 3), we decided that the dosing level for the following treatment study should be maintained at below 42mg/kg/wk as a precaution. We further speculated that this potential toxicity at the higher dose may be related to the SIM/SIM-mPEG micelle's early distribution to the liver (Figure 1). Future



quantitative PK/BD studies will be necessary to provide definitive evidence of this possibility. Regarding the treatment schedule, previous studies have shown that inflammation, tissue swelling, and muscle fiber degeneration are evident 2 days post fracture (19). Based on this timeline, we initiated the treatment in order to optimize the cell-mediated sequestration and uptake of the SIM/SIM-mPEG micelle.

In the therapeutic efficacy study, the data from micro-CT imaging (Figure 4) and analysis (Figure 5.) verified the enhanced callus formation and mineralization in the SIM/SIM-mPEG-treated group compared to the CON in the closed fracture mouse model. The values of the mineralized bone volume fraction (BV/TV), bone surface density (BS/TV) and connectivity density (Conn.D) within the callus in the micelle-treated mice are higher than those of the CON and dose equivalent free SIM-treated (3 mg/kg/day) mice. This low dose free SIM treatment was not able to enhance fracture healing when compared to the CON, whereas high dosage (6 mg/kg/day) of free SIM could only partially improve some of the morphometric parameters. Collectively, these data suggest that when utilized at an optimized dosing level, the systemically administered SIM/SIM-mPEG can effectively potentiate therapeutic efficacy when compared to dose equivalent free SIM in the closed fracture mouse model.

Interestingly, SIM/SIM-mPEG micelles also displayed potent efficacy in the prevention of fracture-associated disuse-induced bone loss in the tibia. Since mechanical stimulation is critical for the maintenance of skeletal integrity and bone mass (21, 22), disuse-induced bone loss is frequently observed in bed-ridden patients associated with skeletal trauma (23). In the current study, mechanical unloading-induced bone loss in the proximal metaphyseal region of the tibia is clearly evident in the lower values of bone mineral density (BMD), bone volume fraction (BV/TV) and trabeculae number (Tb.N) of the CON group. For SIM/SIM-mPEG treated animals, these values are all significantly higher than the CON and SIM groups, which suggests that the treatment can prevent micro-structural deterioration of the bone while free SIM cannot. Based on these findings, we speculate that the improved mobility of the SIM/SIM-mPEG mice may be related to the accelerated femoral fracture healing, rather than any direct effect of SIM. The more rapid restoration of mechanical loading would be expected to suppress bone resorption and activate bone formation, thus preventing bone loss (24). However, the detailed molecular mechanisms involved need to be further investigated in the future.

## 5. CONCLUSION

In this study, we have validated the targeting and the therapeutic efficacy of SIM/SIM-mPEG micelles in a closed fracture mouse model. The micelle dosing level was optimized based upon a preliminary evaluation of dose related toxicity. Additionally, the therapeutic benefits of SIM/SIM-mPEG micelles were observed not only in improving fracture healing, but also in preventing disuse-induced bone loss associated with the trauma. Together with our previous findings, these new data further support the potential clinical translational of SIM/SIM-mPEG micelles as an effective treatment for skeletal fractures.

## Acknowledgments

This study was supported in part by NIH (R01 AR062680) and Nebraska Arthritis Outcome Research Center (NAORC). We thank Mr. Arun Tatiparthi of Micro Photonics for his assistance with the micro-CT analysis. Y.Z. was supported by the Bukey Fellowship from University of Nebraska Medical Center.

## ABBREVIATIONS

<b>ALP</b>	alkaline phosphatase
<b>ALT</b>	alanine aminotransferase
<b>AST</b>	aspartate aminotransferase
<b>BMD</b>	bone mineral density
<b>BUN</b>	blood urea nitrogen
<b>BV/TV</b>	bone volume fraction
<b>BS/TV</b>	bone surface density
<b>CON</b>	vehicle-treated control group
<b>Conn.D</b>	connectivity density
<b>CPK</b>	creatine phosphokinase
<b>DA</b>	degree of anisotropy
<b>Ecc</b>	mean eccentricity
<b>ELVIS</b>	extravasation through leaky vasculature and inflammatory cell-mediated sequestration
<b>FD</b>	fractal dimension
<b>FX</b>	fracture
<b>H&amp;E</b>	hematoxylin and eosin
<b>IACUC</b>	institutional animal care and use committee
<b>micro-CT</b>	micro-computed tomography
<b>MMI</b>	mean polar moment of inertia
<b>NIRF</b>	near infrared fluorescence
<b>PEG</b>	polyethylene glycol
<b>ROI</b>	region of interest
<b>SIM</b>	simvastatin
<b>SIMA</b>	simvastatin acid

<b>SIM/SIM-mPEG</b>	a micellar macromolecular prodrug formulation of simvastatin based on polyethylene glycol
<b>SMI</b>	structure model index
<b>Tb.N</b>	trabecular number
<b>Tb.Pf</b>	trabecular bone pattern factor
<b>Tb.Sp</b>	trabecular separation
<b>Tb.Th</b>	trabecular thickness
<b>TLC</b>	thin layer chromatography
<b>TP</b>	total protein
<b>VOI</b>	volume of interest

## References

1. Dempster DW. Osteoporosis and the burden of osteoporosis-related fractures. The American journal of managed care. 2011; 17(Suppl 6):S164–169. [PubMed: 21761955]
2. Rousculp MD, Long SR, Wang S, Schoenfeld MJ, Meadows ES. Economic burden of osteoporosis-related fractures in Medicaid. Value in health : the journal of the International Society for Pharmacoeconomics and Outcomes Research. 2007; 10:144–152. [PubMed: 17391423]
3. Zhang Y, Bradley AD, Wang D, Reinhardt RA. Statins, bone metabolism and treatment of bone catabolic diseases. Pharmacological research. 2014; 88:53–61. [PubMed: 24407282]
4. Price U, Le HO, Powell SE, Schmid MJ, Marx DB, Zhang Y, Wang D, Narayana N, Reinhardt RA. Effects of local simvastatin-alendronate conjugate in preventing periodontitis bone loss. Journal of periodontal research. 2013; 48:541–548. [PubMed: 23278592]
5. Killen AC, Rakes PA, Schmid MJ, Zhang Y, Narayana N, Marx DB, Payne JB, Wang D, Reinhardt RA. Impact of local and systemic alendronate on simvastatin-induced new bone around periodontal defects. Journal of periodontology. 2012; 83:1463–1471. [PubMed: 22420870]
6. Jia Z, Zhang Y, Chen YH, Dusad A, Yuan H, Ren K, Li F, Fehring EV, Purdue PE, Goldring SR, Daluiski A, Wang D. Simvastatin prodrug micelles target fracture and improve healing. Journal of controlled release : official journal of the Controlled Release Society. 2015; 200:23–34. [PubMed: 25542644]
7. Wangand SR, Goldring D. The bone, the joints and the Balm of Gilead. Molecular pharmaceutics. 2011; 8:991–993. [PubMed: 21800906]
8. Ren K, Purdue PE, Burton L, Quan LD, Fehring EV, Thiele GM, Goldring SR, Wang D. Early detection and treatment of wear particle-induced inflammation and bone loss in a mouse calvarial osteolysis model using HPMA copolymer conjugates. Molecular pharmaceutics. 2011; 8:1043–1051. [PubMed: 21438611]
9. Yuan F, Nelson RK, Tabor DE, Zhang Y, Akhter MP, Gould KA, Wang D. Dexamethasone prodrug treatment prevents nephritis in lupus-prone (NZB x NZW)F1 mice without causing systemic side effects. Arthritis and rheumatism. 2012; 64:4029–4039. [PubMed: 22886616]
10. Yuan F, Quan LD, Cui L, Goldring SR, Wang D. Development of macromolecular prodrug for rheumatoid arthritis. Advanced drug delivery reviews. 2012; 64:1205–1219. [PubMed: 22433784]
11. Skoglund B, Forslund C, Aspenberg P. Simvastatin improves fracture healing in mice. Journal of bone and mineral research : the official journal of the American Society for Bone and Mineral Research. 2002; 17:2004–2008.

12. Bonnarensand TA, Einhorn F. Production of a standard closed fracture in laboratory animal bone. *Journal of orthopaedic research : official publication of the Orthopaedic Research Society*. 1984; 2:97–101. [PubMed: 6491805]
13. Yoshinari M, Matsuzaka K, Hashimoto S, Ishihara K, Inoue T, Oda Y, Ide T, Tanaka T. Controlled release of simvastatin acid using cyclodextrin inclusion system. *Dental materials journal*. 2007; 26:451–456. [PubMed: 17694757]
14. Mundy G, Garrett R, Harris S, Chan J, Chen D, Rossini G, Boyce B, Zhao M, Gutierrez G. Stimulation of bone formation in vitro and in rodents by statins. *Science*. 1999; 286:1946–1949. [PubMed: 10583956]
15. Oryan A, Kamali A, Moshiri A. Potential mechanisms and applications of statins on osteogenesis: Current modalities, conflicts and future directions. *Journal of controlled release : official journal of the Controlled Release Society*. 2015; 215:12–24. [PubMed: 26226345]
16. Ibrahim N, Mohamad S, Mohamed N, Shuid AN. Experimental fracture protocols in assessments of potential agents for osteoporotic fracture healing using rodent models. *Current drug targets*. 2013; 14:1642–1650. [PubMed: 24350807]
17. Holstein JH, Garcia P, Histing T, Kristen A, Scheuer C, Menger MD, Pohlemann T. Advances in the establishment of defined mouse models for the study of fracture healing and bone regeneration. *Journal of orthopaedic trauma*. 2009; 23:S31–38. [PubMed: 19390374]
18. Holstein JH, Matthys R, Histing T, Becker SC, Fiedler M, Garcia P, Meier C, Pohlemann T, Menger MD. Development of a stable closed femoral fracture model in mice. *The Journal of surgical research*. 2009; 153:71–75. [PubMed: 18656902]
19. Manigrassoand JP, O'Connor MB. Characterization of a closed femur fracture model in mice. *Journal of orthopaedic trauma*. 2004; 18:687–695. [PubMed: 15507822]
20. Quan L, Zhang Y, Crielaard BJ, Dusad A, Lele SM, Rijcken CJ, Metselaar JM, Kostkova H, Etrych T, Ulbrich K, Kiessling F, Mikuls TR, Hennink WE, Storm G, Lammers T, Wang D. Nanomedicines for inflammatory arthritis: head-to-head comparison of glucocorticoid-containing polymers, micelles, and liposomes. *ACS nano*. 2014; 8:458–466. [PubMed: 24341611]
21. Manolagas SC. Birth and death of bone cells: basic regulatory mechanisms and implications for the pathogenesis and treatment of osteoporosis. *Endocrine reviews*. 2000; 21:115–137. [PubMed: 10782361]
22. Judex S, Gupta S, Rubin C. Regulation of mechanical signals in bone. *Orthodontics & craniofacial research*. 2009; 12:94–104. [PubMed: 19419452]
23. Jaul E, Malcov T, Menczel J. Osteoporosis in tube-fed bed-ridden elderly female patients. *Journal of the American Geriatrics Society*. 2009; 57:1318–1320. [PubMed: 19570174]
24. Nakamura H, Aoki K, Masuda W, Alles N, Nagano K, Fukushima H, Osawa K, Yasuda H, Nakamura I, Mikuni-Takagaki Y, Ohya K, Maki K, Jimi E. Disruption of NF-kappaB1 prevents bone loss caused by mechanical unloading. *Journal of bone and mineral research : the official journal of the American Society for Bone and Mineral Research*. 2013; 28:1457–1467.

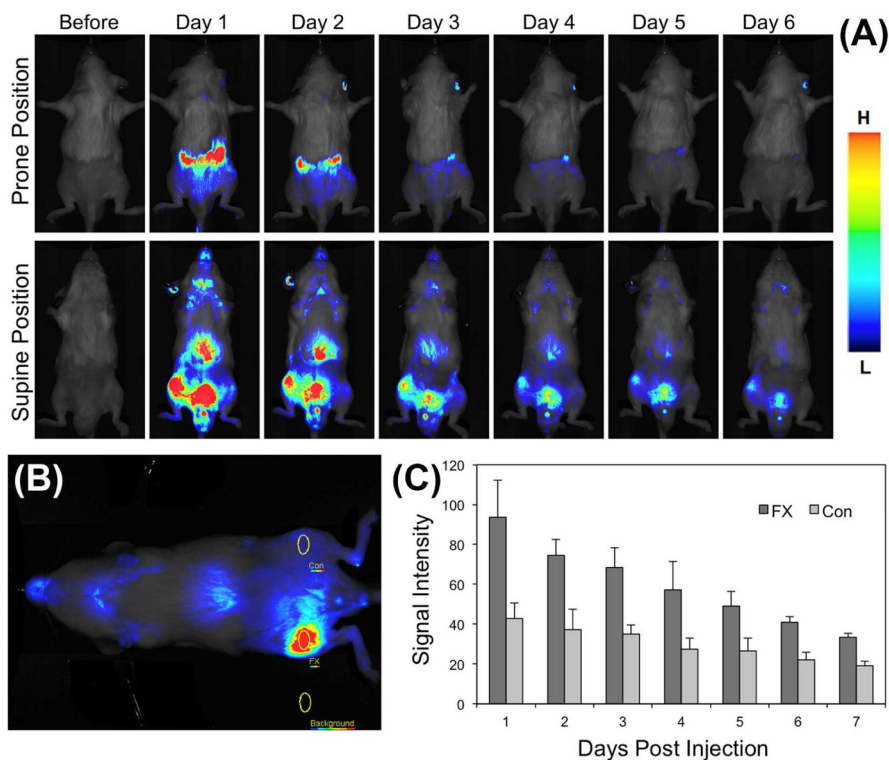


**Figure 1.**

Live optical imaging of SIM/SIM-mPEG micelle's distribution in mice with a closed right femur fracture. IRDye<sup>®</sup> 800CW-labeled SIM/SIM-mPEG was given via tail vein injection on 7th day post-surgeries. Mice were imaged prior and each day after the administration of the labeled micelle for the following 7 days (n=3). (A) According to the sequence of images taken, the fractured femurs demonstrate more intense and longer lasting NIR signals than the intact side. (B) During a semi-quantitative analysis, the NIRF signal intensity from the labeled SIM/SIM-mPEG was measured from a consistent region of interest (yellow circle) at the fracture (FX) site and intact control (Con) site for all the mice. (C) Compared to the intact leg, the fractured side demonstrated more intense NIRF signal in the femoral region. The signal intensity differences between the two sides are statistically significant (t-test,  $P < 0.05$ ).

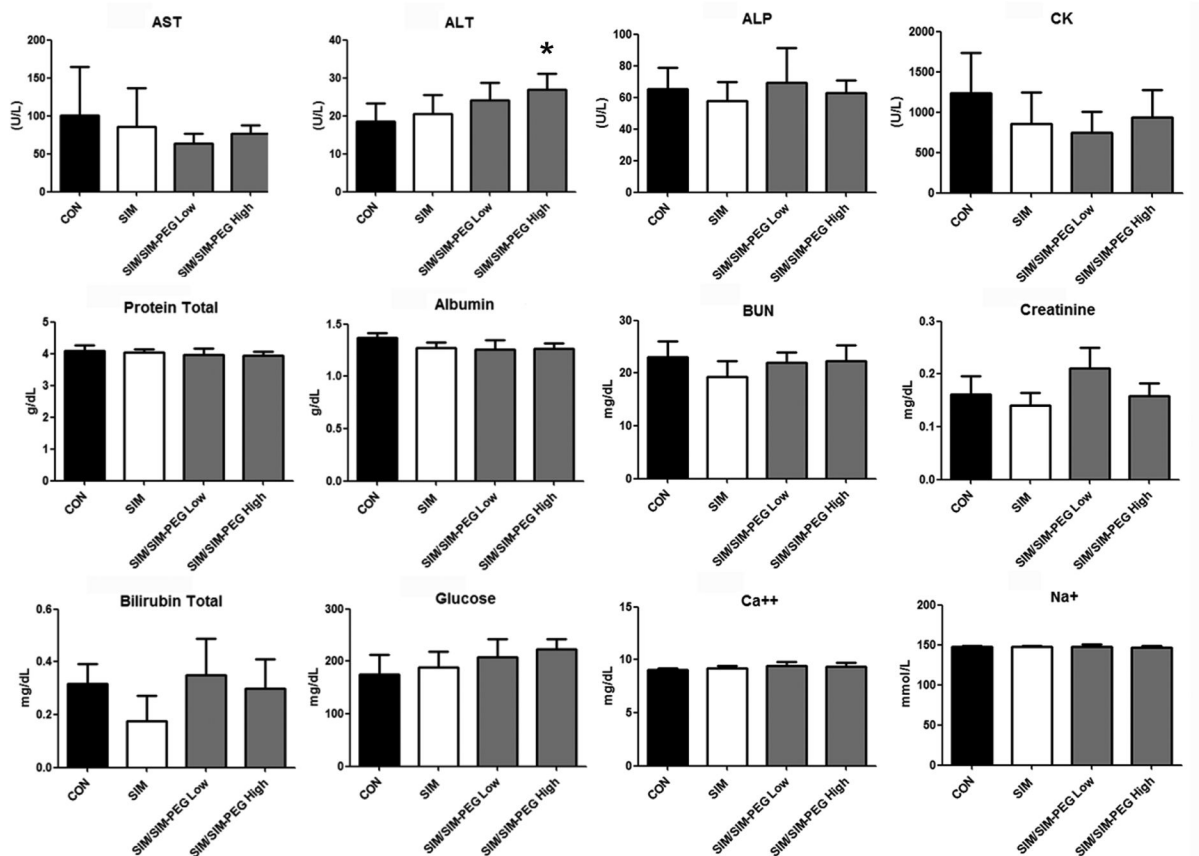


**Figure 2.** Serum biomarkers of fractured mice treated with SIM formulations. \*  $P < 0.05$  vs. CON

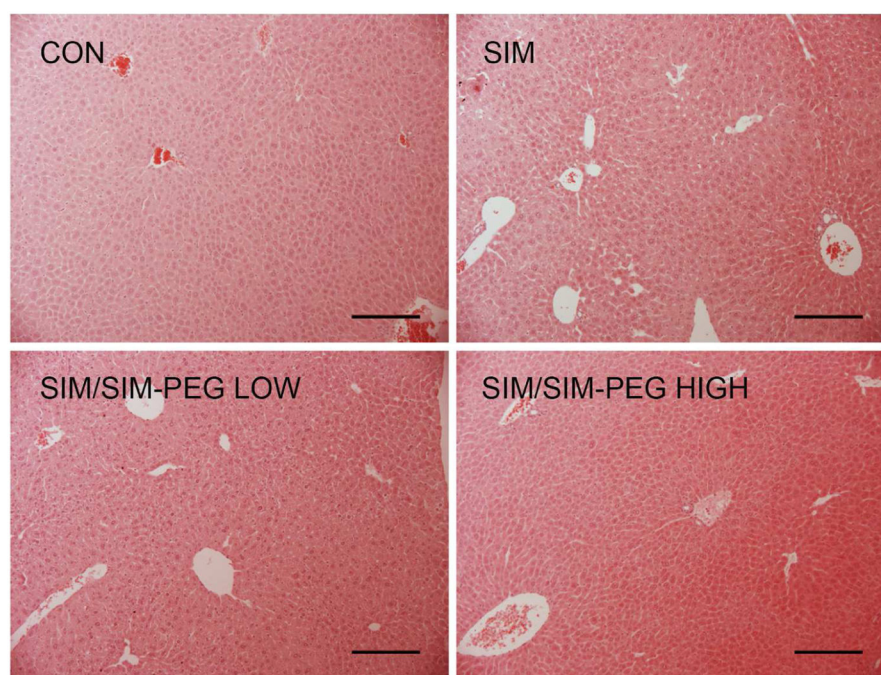


**Figure 3.** Representative histopathologic images (H&E staining,  $\times 10$ ) of livers collected from femur fractured mice treated with different SIM formulations. No apparent histopathologic changes were detected in any of the SIM formulation-treated groups when compared to the CON. Bar = 0.2 mm.

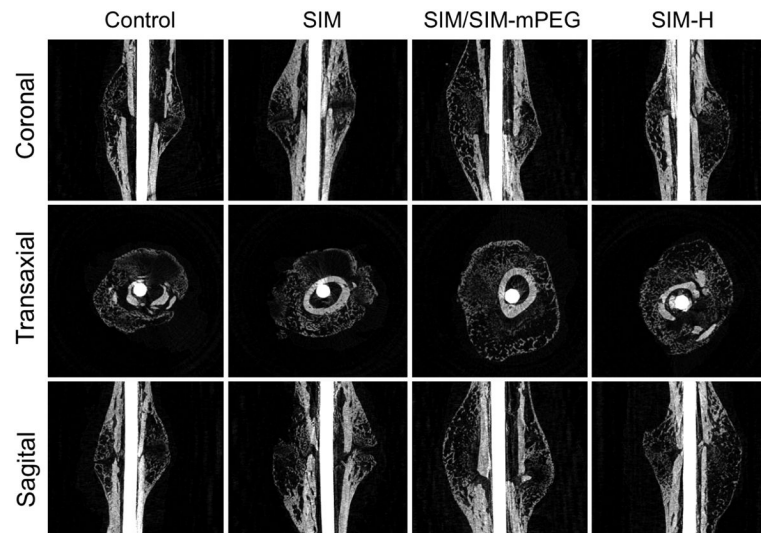


**Figure 4.** Representative micro-CT images of the healing of fractured femurs on day-21 post surgery. The images for each animal group were selected from the animals showing the average values of callus BV/TV during quantitative analysis of the micro-CT data. The SIM/SIM-mPEG treated group exhibited more consolidated and calcified callus formation, compared to the CON- and SIM-treated groups.



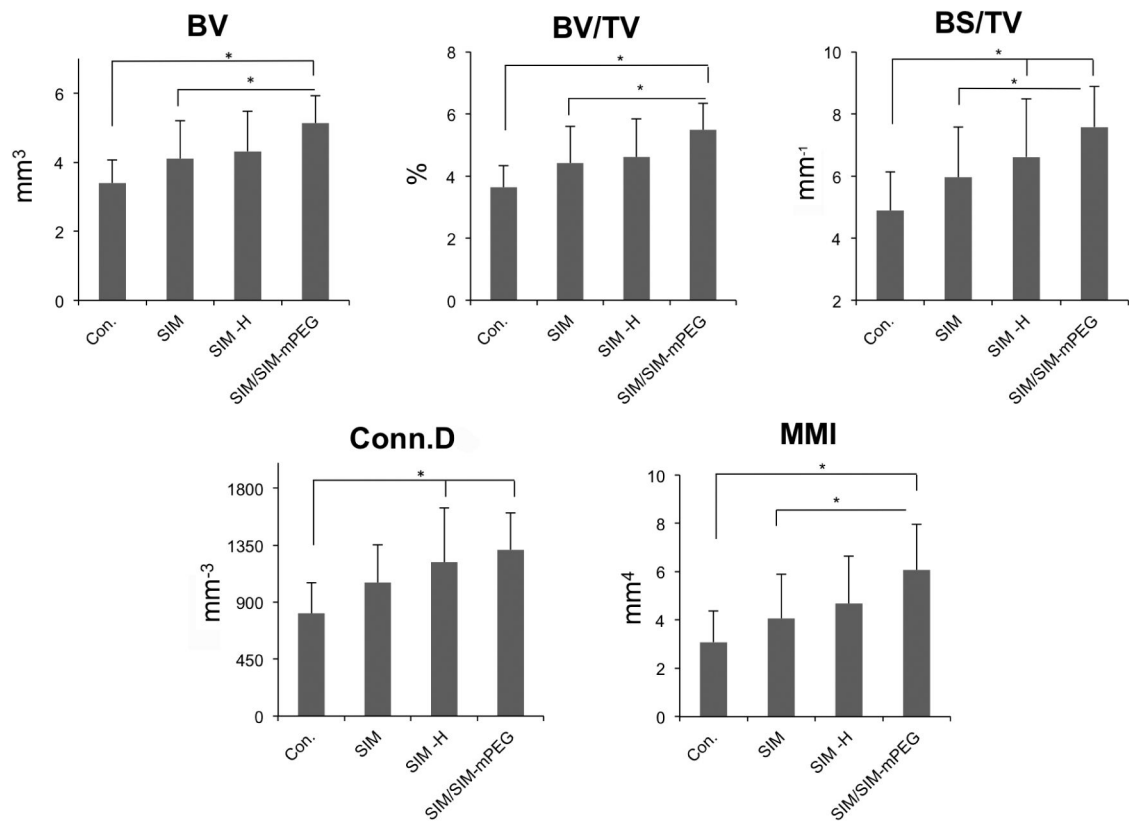


**Figure 5.** Micro-CT morphometric analyses showing the quantitative indices of callus formation. Data is expressed as mean  $\pm$  SD. \*  $P < 0.05$ .

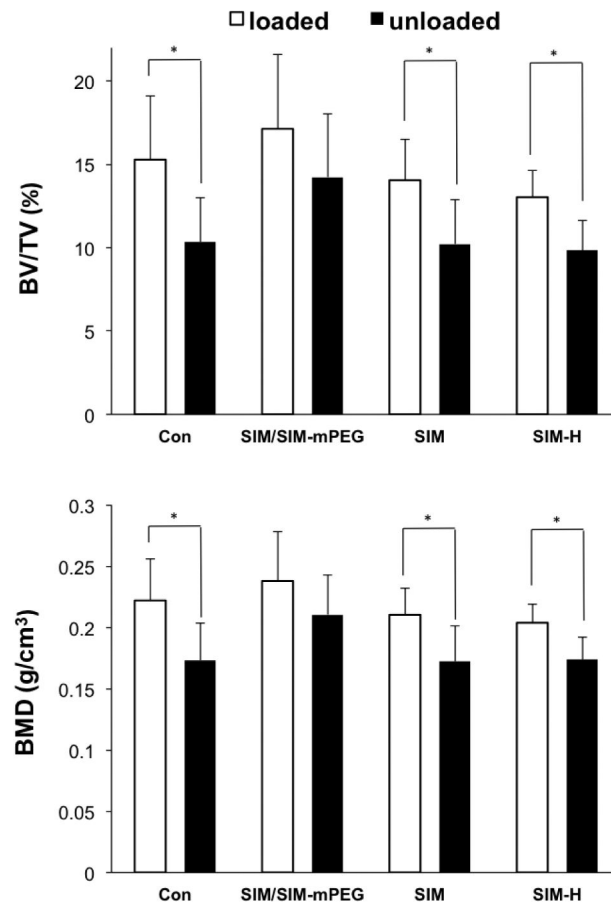


**Figure 6.** SIM/SIM-mPEG suppressed fracture associated unloading-induced bone loss. Micro-CT histomorphometric analysis of the proximal metaphyseal regions of the tibias from the loaded (tibia of intact side, empty box) and unloaded (tibia of fractured side, black box) sides was performed. Data is expressed as mean  $\pm$  SD, \*  $P < 0.05$ .

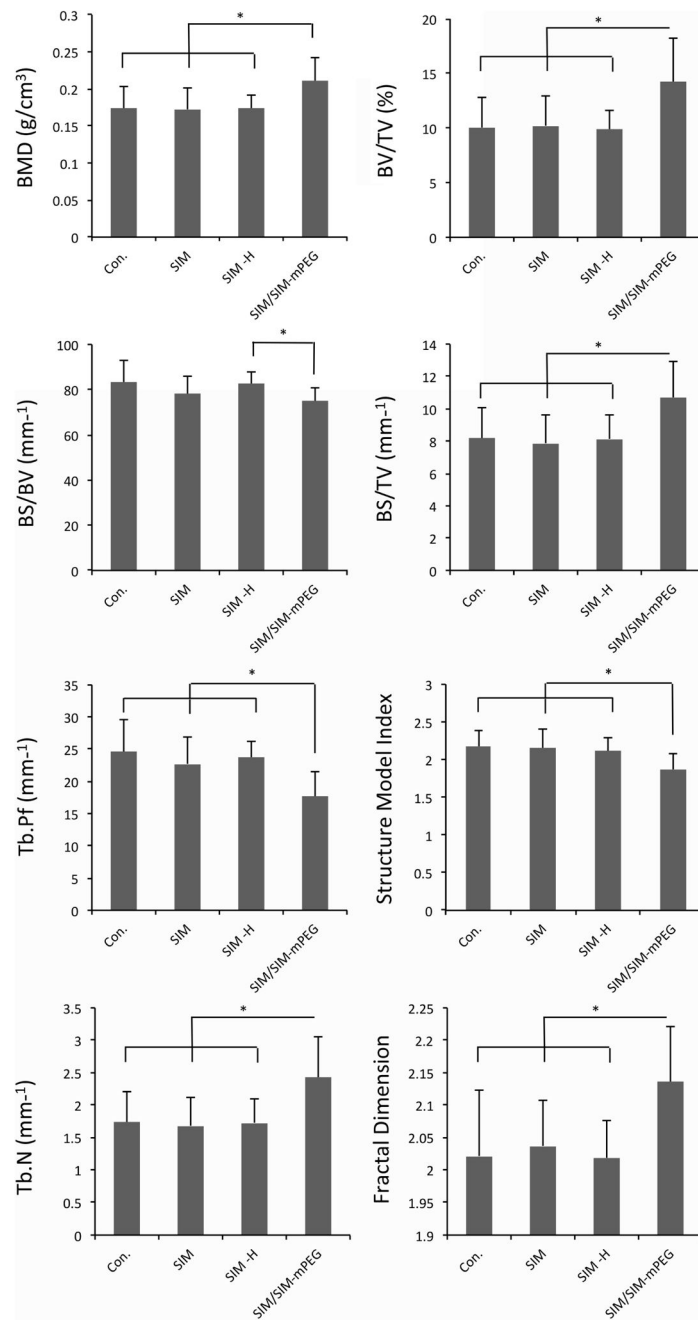
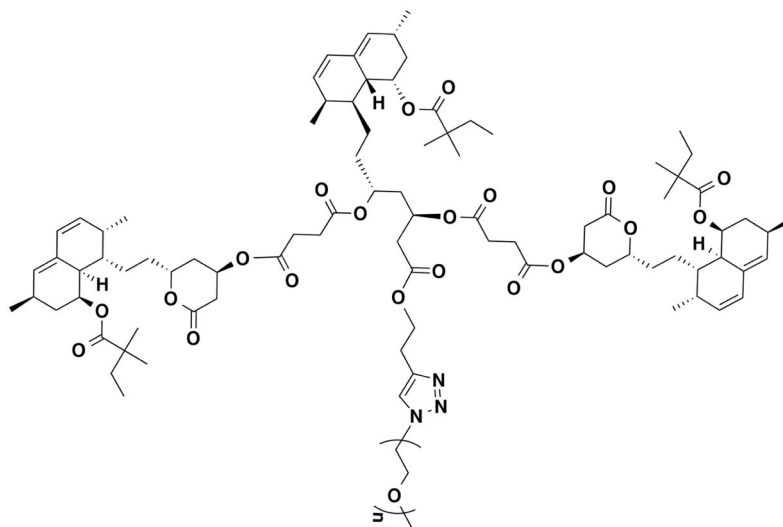
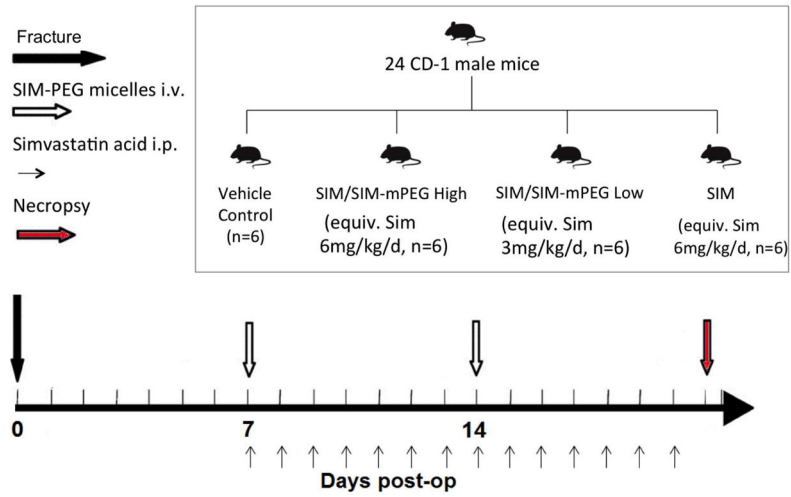


**Figure 7.** SIM/SIM-mPEG rescues micro-structural deterioration in trabecular bone caused by fracture-associated unloading. Micro-CT histomorphometric analysis of the proximal metaphyseal regions of the tibiae from the unloaded (tibiae of fractured side) side was performed. Data is expressed as mean  $\pm$  SD, \*  $P < 0.05$ .

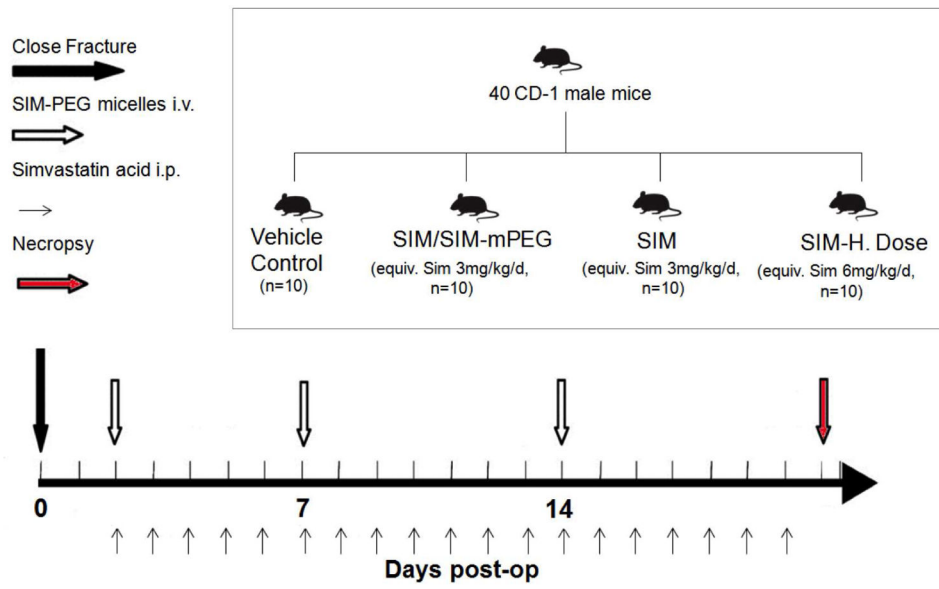


**Scheme 1.**  
Chemical structure of SIM-mPEG.



**Scheme 2.**

Experiment design of the safety evaluation of SIM/SIM-mPEG in a closed fracture mouse model.



**Scheme 3.** Experiment design of the therapeutic study of SIM/SIM-mPEG in a closed fracture mouse model.